Available online at www.sciencedirect.com

ScienceDirect

Procedia Structural Integrity 37 (2022) 439–446

Structural Integrity Procedia

www.elsevier.com/locate/procedia

ICSI 2021 The 4th International Conference on Structural Integrity

Damage assessment of CFRP laminate plate subjected to close-range blast loading: hydrocode methodology validation and case study

A. Vescovini[a], L. Lomazzi[a], M. Giglio[a], A. Manes[a]*

[a]*Politecnico di Milano, Department of Mechanical Engineering, Via La Masa n.1, Milan, Italy*

Abstract

Blast loading represents a critical damaging event in all structures. Although composite materials have been increasingly adopted in structural application, the effect of such dynamic loading event on composite structures is still to be evaluated in detail. This work defines a reliable numerical methodology to assess the damage occurring in carbon fiber reinforced polymer (CFRP) plate subjected to close-range blast loading. The numerical methodology is validated with a benchmark experiment found in literature and is employed to study in detail the damage mechanisms and eventual Fluid Structure Interaction (FSI) effects. The numerical analyses are carried out through a commercially available software package employing two methods, i.e., the ConWep and the hybrid coupled Eulerian-Lagrangia (CEL)-ConWep approaches, and the results from the simulations are compared with experimental evidence from the original work. The results show that (i) the hybrid approach seems to be a promising solution in terms of efficiency and accuracy in modelling blast events, (ii) the ConWep approach accurately reproduces experimental observations, even though such a method has strong limitations.

Keywords: Blast loading; CFRP; Damage.

* Corresponding author. Tel.: +39-02 2399 8474.
E-mail address: alessandro.vescovini@polimi.it

10.1016/j.prostr.2022.01.107

1. Introduction

Composite materials are being widely used in military applications, equipment and assets such as protective panels for armored vehicles, riot shields and military helmets. In this field of application composites structures are at risk from attack using explosive ordnances, so it is worth investigating the response of composite plate-like structures subjected to dynamic loading conditions resulting from a blast event.

Throughout the past decades many experimental research has been carried out on explosive blast loads on laminates (Langdon et al., 2014; Mouritz, 2019) and some included carbon fiber reinforced polymer plates(Comtois et al., 1999; Gargano et al., 2019; Yahya et al., 2011). The blast load depends on many parameters such as the mass and the stand-off distance of the explosive, while the effect on the composite plate depends on the manufacturing features, the geometry and the mechanical properties. The damage, in particular, is strongly dependent on the intralaminar failure stress and the interlaminar properties of the composite laminate. Although being a topic raising interest within researchers, experimental blast tests are expensive, potentially dangerous, and time-consuming to perform; for this reason, modelling the blast response of laminates exploiting numerical simulations offers the opportunity to overcome the inherent limitations of experimental tests. Hence, finite element (FE) analyses are often employed to predict the behavior resulting from dynamic loading from nearby explosion (Mouritz, 2019). FE analyses can model the non-linear and post-failure behavior of composite materials subjected to blast loading, which is known to be crucial to accurately represent the response of a composite structure (Gargano et al., 2019; LeBlanc and Shukla, 2010). However, a limited number of numerical models are found to be validated with experimental observation in the scientific literature (Mouritz, 2019), exceptions are found in the works of (Gargano et al., 2019; Gunaryo et al., 2020) that present a validated FE model of carbon fibre-polymer laminates and of woven glass/epoxy composite plates subjected to blast loading, respectively. In addition most of the papers present the blast load modelled using a pure Lagrangian approach, that is known not to be accurate enough in close-range scenarios (L. Lomazzi et al., 2021) and cannot predict fluid-structure interactions (Aune et al., 2021).

In this work, two methodologies have been used to model blast loading: pure Lagrangian and coupled eulerian-Lagrangian (CEL) approaches. These two methods have been used to replicate the experimental test that is described in the paper of (Gargano et al., 2019) and presented in Section **Error! Reference source not found.**, involving carbon fibre-polymer laminates subjected to blast loading. The methodologies, along with the description of the structural models, are reported in Section **Error! Reference source not found.**. The results, presented in Section **Error! Reference source not found.**, are presented in terms of composite mechanical behavior and damaging and are compared to those of the paper of (Gargano et al., 2019) and to the experimental observations. Finally, the conclusions are drawn in Section **Error! Reference source not found.**.

2. Case study

The experimental test used to benchmark the methodologies proposed in this work are taken from the experimental scenario presented in the work in (Gargano et al., 2019).

In this test a Carbon-Polyester laminate plate was subjected to a blast load generated by the detonation of a 100 g spherical Type 4 plastic explosive charge at 0.4 m standoff distance from the target. The composite plate was constituted by seven plain-woven fabric plies stacked with warps all along the same orientation ([0/90] pattern). The resulting thickness of each ply in the composite was 0.6 mm. The plate had dimensions 275x275 mm^2 and was fixed to a support structure by means of a steel window frame leaving an exposed area of 250x250 mm^2. The frame was lined with soft EPDM 414 foam in the area that overlaps the composite plate, creating simply supported-like boundary conditions.

3. Numerical model

3.1. Blast loading modelling

In this sub-section the two approaches considered to describe the blast load are presented and briefly described.

The first method consists in a pure Lagrangian analysis, in which the blast pressure is predicted exploiting empirical equations and the structure is modelled with Lagrangian elements. The blast pressure is exerted as an analytic pressure load based on specific equation implemented in the software. In particular, the Kingery-Bulmash (KB) equations are exploited to predict the blast load generated by the explosion of High Explosive (HE) material (Kingery and Bulmash, 1984). The equations were obtained via model fitting to experimental results and require only the scaled distance as input value, defined according to an analytical equation (Cranz et al., 1926; Hopkinson, 1915). The analytical pressure applied to the target structure is typically computed according to the equation found in (Randers-Pehrson et al., 1997), where incident and reflected pressure values are estimated by the Kingery-Bulmash equations. The reader is referred to (L Lomazzi et al., 2021) for an accurate discussion on this methodology. The blast loading predicted in this way is considered rather accurate and convenient from a computational perspective, although no fluid structure interaction effects can be considered using this method.

The blast pressure loading is determined employing the keyword *LOAD_BLAST_ENHANCED in LS-Dyna, selecting a spherical free-air burst explosion (BLAST = 2) and defining M = 168 g equivalent TNT weight employing the equations proposed in (Bogosian et al., 2016) that satisfy the equivalence in terms of blast pressure prediction.

The second method to model the blast load consists of modelling the target structure with Lagrangian elements while the HE and the surrounding materials are modelled using Eulerian elements. The Jones-Wilkins-Lee (JWL) equation of state is employed to evaluate the thermodynamic state of the HE material after the detonation (Lee et al., 1968). The surrounding material, i.e., air in this work, needs to be modelled because it is required to propagate the shock wave generated by the detonation. The air domain is governed by the ideal gas equation of state (LSTC, 2018). In this work, a hybrid modelling technique has been adopted to reduce the computational effort that would result from a pure CEL analysis where the whole air domain is modelled. The technique consists of propagating the shock wave far from the plate using the KB equations, then the shock wave is transmitted into the air domain that surrounds locally the target plate.

The air domain was modelled with solid hexahedral elements with characteristic dimension at convergence 1 mm. The formulation selected in this work is the solid section ELFORM = 5, which identifies 1-point Arbitrary Lagrangian-Eulerian (ALE) elements. The keyword *ALE_REFERENCE_SYSTEM_GROUP is employed to model the behavior of the ALE elements with PRTYPE = 8 mesh smoothing option, dedicated to scenarios involving shock waves, and EFAC = 1 initial mesh remapping factor to force pure Eulerian behavior. The card *CONTROL_ALE is included with METH = 3 advection method, AFAC = -1 to turn off smoothing weight factor and EBC = 0 to set flow-out boundary condition. Finally, the reference pressure value applied to the free surfaces of the ALE mesh boundary (PREF field) is set to 101,325 Pa.

The air behavior is modelled using the ideal gas equation of state and the material model MAT_009 (*MAT_NULL) assigning 1.225 $kg \cdot m^{-3}$ density and $1.8 \cdot 10^{-5}$ $Pa \cdot s$ dynamic viscosity ("MU"). The elements acting as receptors for the blast wave are included into a segment set that is specified in the card *LOAD_BLAST_SEGMENT_SET. The parameters included in the *LOAD_BLAST_ENHANCED are the same described above. The interaction between the shock wave propagating in the Eulerian domain and the composite plate is set up employing the card *CONSTRAINED_LAGRANGE_IN_SOLID. The fluid-structure coupling method CTYPE=4 is considered in the analysis, which is a penalty coupling for solid elements without erosion.

Figure 1 presents the two methodologies described above employed to model the blast loading event.

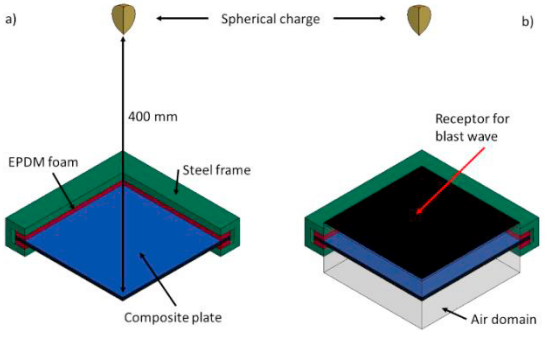

Figure 1: Blast simulation methodology: pure Lagrangian (a) and coupled Eulerian-Lagrangian (b)

3.2. Structural modelling

The target structure is modelled using Lagrangian elements and applying a double symmetry in order to reduce computational time.. Fully integrated solid elements have been chosen since it was verified by the authors that the CEL approach works better with this type of elements. The simulations proving this statement are not reported because they lie outside the scope of this paper.

The composite target has been modelled adopting a macro-homogeneous discretization, i.e., each ply is modelled with a layer of solid elements with 2 mm dimension, as suggested in the work in Gargano et al. (2019) and one element in the thickness. The intra-laminar mechanical properties are defined employing the LS-DYNA® built-in material model defined as MAT_054 (*MAT_ENHANCED_COMPOSITE_DAMAGE). This material model is based on Hashin failure criteria (Hashin, 1980) and allows to describe also woven composite behavior with the 2WAY = 1 flag in the material keyword. The equation governing the ply failure are reported in **Error! Reference source not found.**. The main non-default parameter used in this work are reported in **Error! Reference source not found.**, according to those reported in the work in Gargano et al. (2019). In **Error! Reference source not found.** DFAILT and DFAILC are intentionally set to large values to avoid element deletion and to replicate the same conditions assumed in the simulations of Gargano et al. (2019). In addition, SC was set to a high value in order to avoid its contribution in material failure, according to the paper of Gargano et al. (2019).

Table 1. Woven composite failure criteria.

Failure modes	Criteria	
Tensile failure	$\left(\frac{\sigma_{11}}{X_T}\right)^2 + \beta\left(\frac{\sigma_{12}}{S_C}\right)^2 \geq 1$	(1)
	$\left(\frac{\sigma_{22}}{Y_T}\right)^2 + \beta\left(\frac{\sigma_{12}}{S_C}\right)^2 \geq 1$	(2)
Compressive failure	$\left(\frac{\sigma_{11}}{X_C}\right)^2 \geq 1$	(3)
	$\left(\frac{\sigma_{22}}{X_C}\right)^2 \geq 1$	(4)
Shear failure	$\left(\frac{\sigma_{12}}{S_C}\right)^2 \geq 1$	(5)

Table 2. Carbon-Polyester laminate ply parameters - MAT_054.

Material property	LS-DYNA symbol	Value
Density	RO	1600 kg·m^{-3}
In-plane longitudinal Young modulus	EA	55 GPa
In-plane transversal Young modulus	EB	55 GPa
Out-of-plane Young modulus	EC	7 GPa
In-plane Poisson's ratio	PRBA	0.25
In-plane shear modulus	GAB	4.5 GPa
Out-of-plane shear modulus	GBC	1.8 GPa
Out-of-plane shear modulus	GCA	1.8 GPa
Woven composite failure criteria flag	2WAY	1
Maximum strain value for fiber tension	DFAILT	1
Maximum strain value for fiber compression	DFAILC	-1
Longitudinal compressive strength	XC	240 MPa
Longitudinal tensile strength	XT	680 MPa
Transversal compressive strength	YC	240 MPa
Transversal tensile strength	YT	680 MPa

Shear strength	SC	1000 MPa

The inter-laminar behavior of the composite was accounted for with a contact interaction between adjacent plies. This interaction is based on the Cohesive Zone Model (CZM) theory and it is applied using the keyword *CONTACT_AUTOMATIC_SURFACE_TO_SURFACE_TIEBREAK. The contact algorithm keeps the nodes belonging to the adjacent plies connected until failure occurs; once failure is reached, the interaction between the two delaminated plies is turned into a simple hard-contact interaction. The equation (6) describes the quadratic criterion governing failure, considering both the normal (σ_n) and the shear (τ_s) interlaminar stresses, and in **Error! Reference source not found.** the maximum allowable stresses are reported, according to the work of Gargano et al. (2019).

$$\left(\frac{\sigma_n}{NFLS}\right)^2 + \left(\frac{\tau_s}{SFLS}\right)^2 \geq 1 \qquad (6)$$

Table 3. Properties of the contact interaction between adjacent plies.

Material property	LS-DYNA symbol	Value
Maximum normal stress	NFLS	60 MPa
Maximum shear stress	SFLS	60 MPa

The whole experimental set up was modelled in order to reliably represent this loading condition, because the boundary conditions significantly influence the results (Lomazzi and Vescovini, 2021). Steel was modelled as purely elastic, with the following properties: 7800 kg·m^{-3} density, 203 GPa Young modulus and 0.3 Poisson's ratio. The foam the steel frame was lined with is the soft EPDM 414. Since in the work of Gargano et al. (2019) the parameters in the material model used for it are not reported and to the authors' best knowledge no data is available in the literature about this foam, a different one taken from the work of Zhang et al. (2014) is considered in our case. The authors consider this choice not critical even though, as previously pointed out, the boundary condition the panel is subjected to significantly influences the results in the panel. Solid hexahedral elements with characteristic dimension 2.5mm and single point integration are employed to model the foam material. In order to avoid excessive deformation and numerical analysis instability erosion was added to the foam, occurring at a maximum effective strain equal to 5. The material constitutive law is implemented exploiting the LS-DYNA keyword MAT_057 (*MAT_LOW_DENSITY_FOAM), that is a law dedicated to highly compressible low-density foams, and the input parameters are reported in Table 4; the interested reader is referred to the LS-DYNA® keyword user's manual (Vol. II) for a more detailed description of the model (LSTC, 2018).

Table 4. Parameters of the material of the foam.

Material property	LS-DYNA symbol	Value
Density	RO	63 kg·m^{-3}
Young's modulus	E	8.4 MPa
Nominal stress versus strain curve	LCID	Curve taken from (Zhang et al., 2014)
Hysteretic unloading factor	HU	0.25
Decay constant for creep unloading	BETA	5.0
Viscous coefficient for damping effects	DAMP	0.5
Shape factor for unloading	SHAPE	5.0
Stiffness coefficient for contact interface stiffness	KCON	1150 MPa

4. Results

In this Section the results of the numerical simulations described in the previous section are presented and discussed.

The two methodologies predict similar values of maximum effective pressure: 12,1 MPa and 10,0 MPa for pure-Lagrangian and CEL respectively, and the decay over time of the pressure is identical between the two. This difference

in the pressure-time histories determines predictions of the maximum vertical displacement of the composite plate central point slightly lower in the CEL analysis than in the Lagrangian simulation: 34.3 mm and 30.5 mm for the Langrangian and CEL analyses, respectively; these two are to be compared with the experimentally measured benchmark result from Gargano et al. (2019), i.e., 34.7 mm. The result from the Lagrangian analysis is very similar to the experimental one, while the maximum deflection is underestimated by the CEL analysis; however, both the results are considered acceptable and prove the reliability of the two proposed methodologies. The reader is referred to the work of (Lomazzi and Vescovini, 2021) for detailed treatment of these aspects related to the blast loading.

Figure 2 shows the comparison of the intra-laminar damage reported in the work of Gargano et al. (2019), experimental (a) and numerical (b), and from the numerical analysis described before, pure Lagrangian approach (c) and CEL (d). The picture (a) shows the experimentally observed damage and the dashed red line is meant to underline the area where damage has been seen to occur. Experimentally, the damage is seen in the horizontal and vertical plane along the symmetry planes of the plate and along the two diagonals of the plate. The blue part in the picture (b) is addressed as "ply rupture" in the paper of Gargano et al. (2019) and approximately reproduces the damage along one symmetry plane; according to their simulation no clear definition was given on the failure mode and the damage along the diagonal direction is missing. Likewise, the blue area in the series of picture (c) and (d) shows the damage area from the analysis carried in this work, i.e., the area where the damage criteria described in the Paragraph **Error! Reference source not found.** are met. In the Figure 2, only the more significant plies are reported, as in the analyses different damage modes reasonably occurred more significantly at different positions through the thickness. In addition, only the damage along the x-direction has been reported, since the y-direction is the other preferential direction of the composite showing the same damage pattern. The results from the pure Lagrangian and CEL analyses are basically identical, supporting the validity of the two methods. The uppermost 1st ply presented severe compression damage on the oblique directions, similarly to those observed experimentally; the damage, as the analyses proceeded in the last steps, propagated in the edges of the plate. This last feature is not observed in the experimental picture. Tensile damage is significant in the bottom ply along the same oblique directions observed experimentally, while it is missing in the upper plies according to the analyses; in the bottom plies compressive damage is also found along the edges.

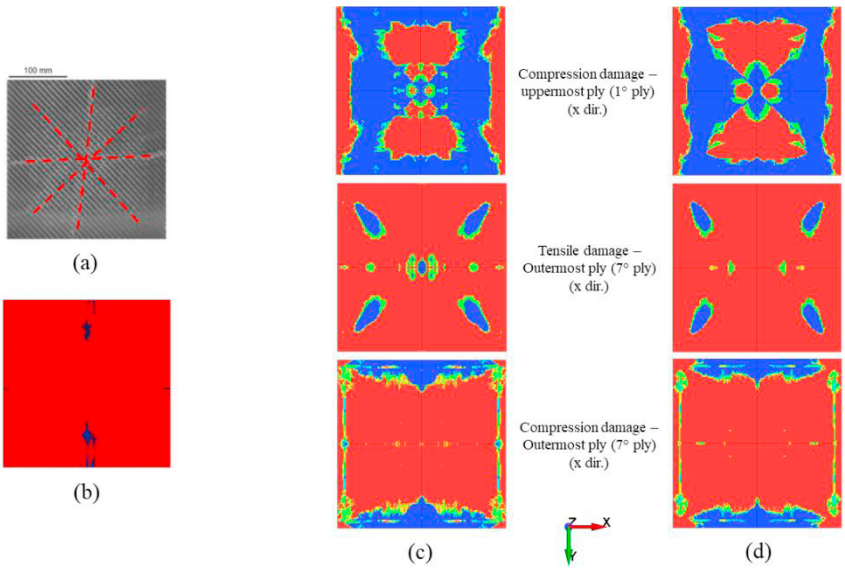

Figure 2: intra-laminar damage comparison from the experimental test (a) and FEM analysis (b) from Gargano et al. (2019), and the pure Lagrangian (c) and CEL (d) analyses from present work.

Figure 3 (a) shows a picture reported in the paper of Gargano et al. (2019) where they noted that a through thickness crack propagated during the blast event. The same interesting patter has been seen also in the analyses of this work in

Figure 3 (b), the blue parts failed by compression damage, although in the real panel the crack propagated with other and different failure mechanisms, such as shear damage and delamination.

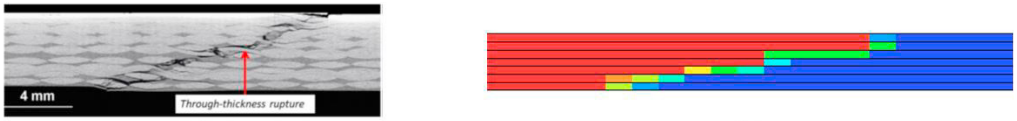

Figure 3: through thickness cracking of composite plate, experimental from Gargano et al. (2019) (a) and numerical analyses (both pure Lagrangian and CEL (b) from present work.

Figure 4 shows the comparison of the inter-laminar damage reported in the work of Gargano et al. (2019), experimental (a) and numerical (b), and from the numerical analysis described above, i.e., the pure Lagrangian approach (c) and the CEL analysis (d). The picture (a) shows experimental damage observed with ultrasound technique, where the blue parts represent inter-laminar damage, the same applies for all the pictures in Figure 4. The picture (b) shows the results reported from the numerical analysis carried out in the paper of Gargano et al. (2019), slight discrepancies are observed from their analysis. Figure 4 (c) and (d) reports the results from the pure Lagrangian and CEL analyses, specifically for the interaction between 1st and 2nd, 4th and 5th, 6th and 7th plies. From our analyses we noted that inter-laminar damage was mostly occurring in the corner of the composite plate where "wrinkles" were seen to occur. It is important to point out that from our analysis severe delamination was seen between the 4th and 5th plies where the composite panel was basically splitting in the middle. The authors believe that this feature that does not coincide with the experimental observations probably because it is related to the importance of accurately defining the boundary condition of the composite panel, i.e. the properties of the rubber foam liner, that significantly influence the inter-laminar damage, but most likely also the intra-laminar one, probably and apparently in a lesser extent.

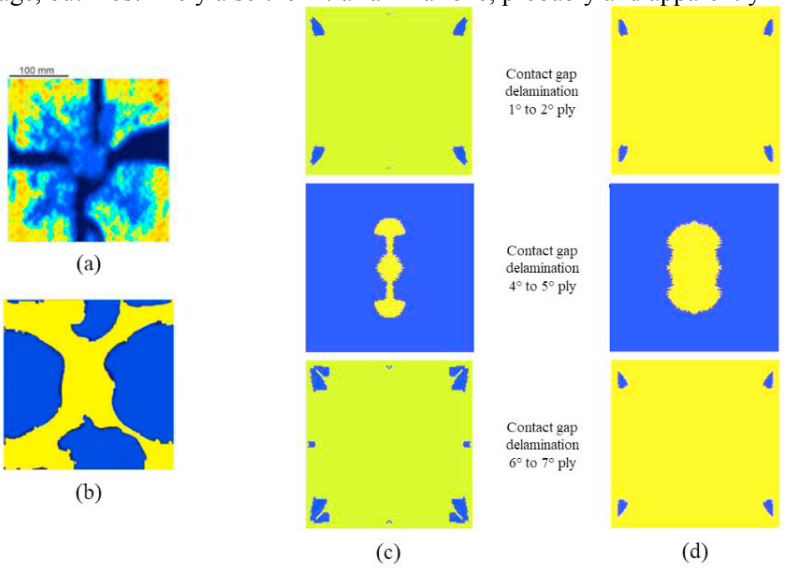

Figure 4: inter-laminar damage comparison from the experimental test (a) and FEM analysis (b) from Gargano et al. (2019), and the pure Lagrangian (c) and CEL (d) analyses from present work.

5. Conclusion

The pure Lagrangian and CEL methods to simulate blast loading are validated and efficient to represent this event, in fact from the results discussed the pressure exerted and the resulting maximum deflection are in agreement with the experimental observation and the paper this work is based on. The damage reported from the pure Lagrangian and CEL methods are comparable with those from the paper of Gargano et al. (2019), yet the authors are aware that

improvements can be made in the representation of blast induced damage by improving and refining the modelling of the materials involved; the composite plate can be model with more advanced and accurate material models and, as already underlined in the discussion, represent accurately the mechanical behavior of the other materials involved in the experimental test is regarded as crucial. Further analyses are foreseen in order to improve damage representation, by investigating other material models for intra-laminar damage and methods for inter-laminar damage.

To conclude, blast secondary effects can possibly be considered in future works to obtain a comprehensive description of the phenomena occurring induced by the blast event.

6. References

Aune, V., Valsamos, G., Casadei, F., Langseth, M., Børvik, T., 2021. Fluid-structure interaction effects during the dynamic response of clamped thin steel plates exposed to blast loading. Int. J. Mech. Sci. 195, 106263.

Bogosian, D., Yokota, M., Rigby, S., 2016. TNT EQUIVALENCE OF C-4 AND PE4: A REVIEW OF TRADITIONAL SOURCES AND RECENT DATA.

Comtois, J.L.R., Edwards, M.R., Oakes, M.C., 1999. The effect of explosives on polymer matrix composite laminates. Compos. Part A Appl. Sci. Manuf. 30, 181–190.

Cranz, K.J., von Eberhard, O., Becker, K.E., 1926. Lehrbuch der Ballistik. Ergänzungen zum Band II [WWW Document].

Gargano, A., Das, R., Mouritz, A.P., 2019. Finite element modelling of the explosive blast response of carbon fibre-polymer laminates. Compos. Part B Eng. 177, 107412.

Gunaryo, K., Heriana, H., Sitompul, M.R., Kuswoyo, A., Hadi, B.K., 2020. Experimentation and numerical modeling on the response of woven glass/epoxy composite plate under blast impact loading. Int. J. Mech. Mater. Eng. 2020 151 15, 1–9.

Hashin, Z., 1980. Failure criteria for unidirectional fiber composites. J. Appl. Mech. 47, 329–334.

Hopkinson, B., 1915. British ordnance board minutes, Report 13565.

Kingery, C., Bulmash, G., 1984. Airblast Parameters from TNT Spherical Air Burst and Hemispherical Surface Burst.

Langdon, G.S., Cantwell, W.J., Guan, Z.W., Nurick, G.N., 2014. The response of polymeric composite structures to air-blast loading: a state-of-the-art. http://dx.doi.org/10.1179/1743280413Y.0000000028 59, 159–177.

LeBlanc, J., Shukla, A., 2010. Dynamic response and damage evolution in composite materials subjected to underwater explosive loading: An experimental and computational study. Compos. Struct. 92, 2421–2430.

Lee, E.L., Hornig, H.C., Kury, J.W., 1968. ADIABATIC EXPANSION OF HIGH EXPLOSIVE DEPOMAPION PRODUCTS.

Lomazzi, L., Giglio, M., Manes, A., 2021. Analytical and empirical methods for the characterisation of the permanent transverse displacement of quadrangular metal plates subjected to blast load: Comparison of existing methods and development of a novel methodological approach. Int. J. Impact Eng. 154, 103890.

Lomazzi, L, Giglio, M., Manes, A., 2021. Analysis of the blast wave-structure interface phenomenon in case of explosive events.

Lomazzi, L., Vescovini, A., 2021. Numerical study on the influence of boundary conditions on the blast response of composite plates. IOP Conf. Ser. Mater. Sci. Eng.

LSTC, 2018. LS-DYNA Keyword User's Manual II.

Mouritz, A.P., 2019. Advances in understanding the response of fibre-based polymer composites to shock waves and explosive blasts. Compos. Part A Appl. Sci. Manuf. 125, 105502.

Randers-Pehrson, G., Bannister, K.A., Qxuaij, L.C., 1997. Airblast Loading Model for DYNA2D and DYNA3D.

Yahya, M.Y., Cantwell, W.J., Langdon, G.S., Nurick, G.N., 2011. The blast resistance of a woven carbon fiber-reinforced epoxy composite: http://dx.doi.org/10.1177/0021998310376103 45, 789–801.

Zhang, T.G., Satapathy, S.S., Dagro, A.M., McKee, P.J., 2014. Numerical Study of Head/Helmet Interaction due to Blast Loading. ASME Int. Mech. Eng. Congr. Expo. Proc. 3 A.